

Big Bang Nucleosynthesis and Particle Dark Matter

Karsten Jedamzik^(a) and Maxim Pospelov^(b,c)

^(a) Laboratoire de Physique Théorique et Astroparticules, UMR5207-CNRS,
Université Montpellier II, F-34095 Montpellier, France,

^(b) Department of Physics and Astronomy, University of Victoria, Victoria, BC, V8P
1A1 Canada

^(c) Perimeter Institute for Theoretical Physics, Waterloo, Ontario N2J 2W9, Canada

E-mail:

jedamzik@lpta.univ-montp2.fr

pospelov@uvic.ca

Abstract.

We review how our current understanding of the light element synthesis during the Big Bang Nucleosynthesis era may help shed light on the identity of particle dark matter.

1. Introduction

In the late 40s and throughout the 50s a number of visionary scientists including Alpher, Fermi, Follin, Gamow, Hayashi, Herman, and Turkevich attempted to explain nuclear abundance patterns observed in the nearby Universe, such as the peculiar high helium mass fraction $Y_p \approx 0.25$. This initially speculative work on an era of nucleosynthesis (element formation) in an expanding Universe at very high temperature $T \sim 10^9\text{K}$ developed slowly but steadily over the coming decades into what is now known as the standard model of Big Bang nucleosynthesis (BBN). The idea that the Universe may have undergone a very hot and dense early phase got triggered by the observations of Hubble in the 1920s, of the recession velocity of galaxies being proportional to their inferred distance from the Milky Way, which were most elegantly explained by a Universe in expansion. The "expanding, hot Big Bang" idea received further support by the observation of the cosmic microwave background radiation (CMBR) by Penzias and Wilson in 1965, believed to be the left-over radiation of the early Universe. Detailed observational and theoretical studies of BBN as well as the CMBR and the Hubble flow have developed into the main pillars on which present day cosmology rests.

BBN takes place between eras with (CMBR) temperatures $T \simeq 3\text{MeV}$ and $T \simeq 10\text{keV}$, in the cosmic time window $t \simeq 0.1 - 10^4\text{sec}$, and may be characterized as a freeze-out from nuclear statistical equilibrium of a cosmic plasma at very low $\sim 10^{-9}$ baryon-to-photon number ratio (cf. Section 2), conditions which are not encountered in stars. It produces the bulk of ^4He and ^2H (D), as well as good fractions of ^3He

and ${}^7\text{Li}$ observed in the current Universe, whereas all other elements are believed to be produced either by stars or cosmic rays. In its standard version it assumes a Universe expanding according the laws of general relativity, at a given homogeneously distributed baryon-to-photon ratio η_b , with only Standard Model particle degrees of freedom excited, with negligible $\mu_l \ll T$ lepton chemical potentials, and in the absence of any significant perturbations from primordial black holes, decaying particles, etc. By a detailed comparison of observationally inferred abundances (cf. Section 3) with those theoretically predicted, fairly precise constraints/conclusions about the cosmic conditions during the BBN era may thus be derived. BBN has been instrumental, for example, in constraining the contribution of extra "degrees of freedom" excited in the early Universe to the total energy density, such as predicted in many models of particle physics beyond the standard model. Such contributions may lead to an enhanced expansion rate at $T \sim 1 \text{ MeV}$ implying an increased ${}^4\text{He}$ mass fraction. It is now known that aside from baryons and other subdominant components not much more than the already known relativistic degrees of freedom (i.e. photons γ 's, electrons and positrons e^\pm 's, and three left-handed neutrinos ν 's) could have been present during the BBN era. BBN is also capable of constraining very sensitively any non-thermal perturbations as induced, for example, by the residual annihilation of weak scale dark matter particles (Section 5), or by the decay of relic particles (Section 7) and the possible concomitant production of dark matter. Moreover, the sheer presence of negatively charged or strongly-interacting weak mass-scale particles during BBN (Section 6) may lead to dramatic shifts in yields of light element through the catalytic phenomena. BBN may therefore constrain properties and production mechanisms of dark matter particles, and this chapter aims at revealing this connection.

It is possible that the biggest contribution of BBN towards understanding the dark matter enigma has already been made. Before the advent of precise estimates of the fractional contribution of baryons to the present critical density, $\Omega_b \approx (0.02273 \pm 0.00062)/h^2$, where h is the Hubble constant in units $100 \text{ km s}^{-1}\text{Mpc}^{-1}$, by detailed observations and interpretations of the anisotropies in the CMBR [1], BBN was the only comparatively precise mean to estimate Ω_b . As it was not clear if the "missing" dark matter was simply in form of brown dwarfs, white dwarfs, black holes (formed from baryons), and/or $T \sim 10^6\text{K}$ hot gas, various attempts to reconcile a BBN era at large $\Omega_b \sim 1$ with the observationally inferred light element abundances were made. These included, for example, BBN in a baryon-inhomogeneous environment, left over possibly due to a first-order QCD phase transition at $T \approx 100 \text{ MeV}$, or BBN with late-decaying particles, such as the supersymmetric gravitino (for reviews, cf. [2, 3, 4]). Only continuous theoretical efforts of this sort, and their constant "failure" to account for large Ω_b , gave way to the notion that the dark matter must be in form of "exotic", non-baryonic material, such as a new fundamental particle investigated in the present book.

2. Standard BBN - theory

Standard BBN (SBBN) theory is well understood and described in detail in many modern cosmology text books. The essence of SBBN is represented by a set of Boltzmann equations that may be written in the following schematic form:

$$\frac{dY_i}{dt} = -H(T)T \frac{dY_i}{dT} = \sum (\Gamma_{ij}Y_j + \Gamma_{ikl}Y_kY_l + \dots), \quad (1)$$

where $Y_i = n_i/s$ are the time t (or temperature T) dependent ratios between number density n_i and entropy density s of light elements $i = {}^1\text{H}$, n , D , ${}^4\text{He}$, etc.; the $\Gamma_{ij\dots}$ are generalized rates for element interconversion and decay that can be estimated by experiments and/or theoretical calculations, and $H(T)$ is the temperature-dependent Hubble expansion rate. The system of equations (1) assumes thermal equilibrium *e.g.* Maxwell-Boltzmann distributions for nuclei, which is an excellent approximation maintained by frequent interactions with the numerous γ 's and e^\pm 's in the plasma. The initial conditions for this set of equations are well-specified: for temperatures much in excess of the neutron-proton mass difference, neutron and proton abundances are equal and related to the baryon to entropy ratio, $Y_{neutron} \simeq Y_{proton} \simeq \frac{1}{2}n_{baryon}/s$, while the abundance of all other elements is essentially zero. At temperatures relevant to BBN, the baryonic contribution to the Hubble rate is minuscule, and $H(T)$ is given by the standard radiation-domination formula:

$$H(T) = T^2 \times \left(\frac{8\pi^3 g_* G_N}{90} \right)^{1/2}, \quad \text{where } g_* = g_{boson} + \frac{7}{8}g_{fermion}, \quad (2)$$

with the g 's denoting the excited relativistic degrees of freedom. This expression needs to be interpolated in a known way across the brief epoch of the electron-positron annihilation, after which the photons become slightly hotter than neutrinos and $H(T) \simeq T_9^2/(178 \text{ s})$, where T_9 is the photon temperature in units of 10^9K . A number of well-developed integration routines that go back to an important work of Wagoner, Fowler, and Hoyle [5], allow to solve the BBN system of equations numerically and obtain the freeze-out values of the light elements. A qualitative "computer-free" insight to these solutions can be found in *e.g.* Ref. [6].

In a nutshell, SBBN may be described as follows. After all weak rates fall below the Hubble expansion rate, the neutron-to-proton ratio freezes to $\sim 1/6$, subject to a slow further decrease to $\sim 1/7$ by $T_9 \simeq 0.85$ via neutron decay and out-of-equilibrium weak conversion. At this point, to a good approximation, all neutrons available will be incorporated into ${}^4\text{He}$, since it is the light element with the highest binding energy per nucleon. Synthesis of ${}^4\text{He}$, and all other elements, has to await the presence of significant amounts of D (the "deuterium bottleneck"). This occurs rather late, at $T_9 \simeq 0.85$, since at higher T_9 the fragile D is rapidly photodisintegrated by the multitude of CMBR photons. At $T_9 \lesssim 0.85$ the fairly complete nuclear burning of all D then results in only trace amounts $O(10^{-5})$ of D (and ${}^3\text{He}$) being leftover after SBBN has ended. Elements with nucleon number $A > 4$ are even less produced due to appreciable Coulomb barrier suppression at such low T_9 , resulting in only $O(10^{-10})$ of ${}^7\text{Li}$, and abundances of other

isotopes even lower. SBBN terminates due to the combination of a lack of free neutrons and the importance of Coulomb barriers at low T . In the following a few more details are given:

$O(0.1)$ abundances: ${}^4\text{He}$. The ${}^4\text{He}$ mass fraction Y_p is dependent on the *timing* of major BBN events, such as the neutron-to-proton freeze-out at $T \simeq 0.7$ MeV, post-freezeout neutron depletion before the deuterium bottleneck, and the position of this bottleneck itself as a function of temperature. Consequently, Y_p is dependent on such well-measured quantities as Newton's constant, the neutron-proton mass difference, neutron lifetime, deuterium binding energy, and to a much lesser degree on less precisely known values for the nuclear reaction rates. This sensitivity to the timing of the BBN events makes ${}^4\text{He}$ an important probe of the Hubble expansion rate, and of all possible *additional* non-standard contributions that could modify it. The SBBN predicts Y_p with an impressive precision, $Y_p = 0.2486 \pm 0.0002$, where we use the most recent evaluation [7].

$O(10^{-5})$ abundances: D and ${}^3\text{He}$. Deuterium and ${}^3\text{He}$ BBN predictions are more sensitive both to nuclear physics and to η_b input. Reactions involving these elements are well measured, and with the current WMAP input SBBN is capable of making fairly precise predictions of these abundances: $\text{D}/\text{H} = 2.49 \pm 0.17 \times 10^{-5}$; ${}^3\text{He}/\text{H} = (1.00 \pm 0.07) \times 10^{-5}$.

$O(10^{-10})$ abundances: ${}^7\text{Li}$. Among all observable BBN abundances, ${}^7\text{Li}$ is the most sensitive to the η_b and nuclear physics inputs. The actual observable that BBN predicts is the combined abundance of ${}^7\text{Li}$ and ${}^7\text{Be}$, as later in the course of the cosmological evolution ${}^7\text{Be}$ is transformed into ${}^7\text{Li}$ via electron capture. At the CMBR-measured value of the baryon-to-photon ratio η_b , more than 90% of primordial lithium is produced in the form of ${}^7\text{Be}$ in the radiative capture process, ${}^4\text{He} + {}^3\text{He} \rightarrow {}^7\text{Be} + \gamma$. As the rate for this process per each ${}^3\text{He}$ nucleus is much slower than the Hubble rate, the output of ${}^7\text{Be}$ is almost linearly dependent on the corresponding S -factor for this reaction. With recent improvement in its experimental determination [8, 9, 10], the current $\sim 15\%$ accuracy prediction for ${}^7\text{Be} + {}^7\text{Li}$ stands at $5.24_{-0.67}^{+0.71} \times 10^{-10}$ [7].

$O(10^{-14})$ and less abundances: ${}^6\text{Li}$ and $A \geq 9$ elements. ${}^6\text{Li}$ is formed in the BBN reaction



which at BBN temperatures is \sim four orders of magnitude suppressed relative to other radiative capture reactions such as ${}^4\text{He} + {}^3\text{H} \rightarrow {}^7\text{Li} + \gamma$, and \sim seven/eight orders of magnitude suppressed relative to other photonless nuclear rates. The reason for the extra suppression is in a way accidental: it comes from the same charge to mass ratio for ${}^4\text{He}$ and D, which inhibits the E1 transition, making this radiative capture extremely inefficient. This results in $O(10^{-14})$ level prediction for primordial ${}^6\text{Li}$ which is well below the detection capabilities. Heavier elements with $A \geq 9$ such as ${}^9\text{Be}$, ${}^{10}\text{B}$ and ${}^{11}\text{B}$ are never made in any significant quantities in the SBBN framework, and the main reason for that is the absence of stable $A = 8$ nuclei, as ${}^8\text{Be}$ is underbound by 92 keV

and decays to two α .

3. Observed light element abundances

In the following, we will briefly discuss the observationally inferred light elements, element by element. Here the discussion will also include isotopes, or isotope ratios, such as ${}^6\text{Li}$, ${}^9\text{Be}$, and ${}^3\text{He}/{}^2\text{H}$, which are not always considered in SBBN, but which are very useful to constrain deviations from SBBN.

3.1. ${}^4\text{He}$

The primordial ${}^4\text{He}/\text{H}$ ratio is inferred from observations of hydrogen- and helium-emission lines in extragalactic low-metallicity HII-regions and compact blue galaxies, illuminated by young star clusters. Two particular groups have performed such analysis for years now, with their most recent results $Y_p \approx 0.2477 \pm 0.0029$ [11] and $Y_p \approx 0.2516 \pm 0.0011$ [12]. These estimates are (surprisingly) considerably larger than earlier estimates by both groups (i.e. 0.239 and 0.242, respectively), explained in large parts by a new estimate for HeI emissivities [13]. Other differences with respect to older studies, and/or between the two new studies themselves, are the adopted rates for collisional excitation of H- (He-) emission lines, corrections for a temperature structure in these galaxies ("temperature variations"), corrections for the presence of neutral ${}^4\text{He}$ ("icf - ionisation corrections"), as well as corrections for troughs in the stellar spectra at the position of the ${}^4\text{He}$ - (H-) emission lines ("underlying stellar absorption"). All of these may have impact on the $\gtrsim 1\%$ level. This, as well as the comparatively large change from earlier estimates (coincidentally going into the direction of agreement with the SBBN prediction of $Y_p \approx 0.248$), implies that a conservative estimate $Y_p \approx 0.249 \pm 0.009$ [14] (see also $Y_p \approx 0.250 \pm 0.004$) [15] of the error bar, maybe more appropriate when constraining perturbations of SBBN.

3.2. D

For the observational determination of primordial D/H-ratios high-resolution observations of low-metallicity quasar absorption line systems (QALS) are employed (cf. [16, 17, 18, 19, 20]). QALS are clouds of partially neutral gas which fall on the line of sight between the observer and a high-redshift quasar. The neutral component in these clouds yields absorption features, for example, at the redshifted position of the Lyman- α wavelength. For the very rare QALS of sufficiently simple velocity structure, one may compare the absorption at the Lyman- α position of H with that of D (shifted by 81 km s^{-1}) to infer a D/H ratio. Here the low metallicity of these QALS is conducive to make one believe that stellar D destruction in such clouds is negligible. Currently there exist only about 6 – 8 QALS with D/H determinations. When averaged they yield typical $2.68 - 2.82 \times 10^{-5}$ [19, 21, 22, 20] for the central value, with inferred statistical 1σ error bars of $0.2 - 0.3 \times 10^{-5}$, comparing favorably to the SBBN prediction

of $2.49 \pm 0.17 \times 10^{-5}$ [7] at the WMAP inferred η_b . Nevertheless, as an important cautionary remark, the various inferred D/H ratios in QALS show a spread considerably larger than that expected from the above quoted error bars only. This is usually a sign of the existence of unknown systematic errors. Until these systematics are better understood should primordial values as high as $D/H \approx 4 \times 10^{-5}$ therefore not considered to be ruled out.

3.3. ${}^3\text{He}/D$

Observational determinations of ${}^3\text{He}/H$ -ratios are possible within our galaxy which is chemically evolved. The chemical evolution of ${}^3\text{He}$ is, however, rather involved, with ${}^3\text{He}$ known to be produced in some stars and destroyed in others. Furthermore, any D entering stars will be converted to ${}^3\text{He}$ by proton burning. The net effect of all this is an observed approximate constancy of $(D+{}^3\text{He})/H \approx 3.6 \pm 0.5 \times 10^{-5}$ [23] over the last few billion years in our galaxy. Whereas the relation of galactic observed ${}^3\text{He}/H$ ratios to the primordial one is obscure, the ratio of ${}^3\text{He}/D$ as observed in the presolar nebulae is invaluable in constraining perturbations of SBBN. This ratio $0.83^{+0.53}_{-0.25}$ [23] (where the error bars are obtained when using the independent 2σ ranges of ${}^3\text{He}/H$ and D/H) provides a firm upper limit on the primordial ${}^3\text{He}/D$ [24]. This is because ${}^3\text{He}$ may be either produced or destroyed in stars, while D is always destroyed, such that the cosmological ${}^3\text{He}/D$ ratio may only grow in time.

3.4. ${}^7\text{Li}$

${}^7\text{Li}/H$ ratios may be inferred from observations of absorption lines (such as the 6708Å doublet) in the atmospheres of low-metallicity galactic halo stars. When this is done for stars at low metallicity $[Z]$, ${}^7\text{Li}/H$ ratios show a well-known anomaly (with respect to other elements), i.e. ${}^7\text{Li}/H$ ratios are constant over a wide range of (low) $[Z]$ and some range of temperature (the "Spite plateau"). As most elements are produced by stars and/or cosmic rays, which themselves produce metallicity, the ${}^7\text{Li}$ Spite plateau is believed to be an indication of a primordial origin of this isotope. This interpretation is strengthened by the absence of any observed scatter in the ${}^7\text{Li}$ abundance for such stars. There have been several observational determinations of the ${}^7\text{Li}$ abundance on the Spite plateau. Most of them fall in the range ${}^7\text{Li}/H \approx 1 - 2 \times 10^{-10}$ such as $1.23^{+0.68}_{-0.32} \times 10^{-10}$ [25, 26] and $1.1 - 1.5 \times 10^{-10}$ [27], with some being somewhat higher such as $2.19 \pm 0.28 \times 10^{-10}$ [28]. Here differences may be due to differing methods of atmospheric temperature estimation. These values should be compared to the SBBN prediction $5.24^{+0.71}_{-0.67} \times 10^{-10}$ [7] (with 1σ error estimates), clearly indicating a conflict which is often referred to as the "lithium problem". It is essentially ruled out that this problem be solved by, either, an erroneous atmospheric temperature determination, or significant changes in ${}^7\text{Li}$ producing/destroying nuclear SBBN rates. There remain only two viable possibilities of a resolution to this statistically significant $(4 - 5)\sigma$ problem. First, it is conceivable that atmospheric ${}^7\text{Li}$ has been partially destroyed in such stars due

to nuclear burning in the stellar interior. Though far from understood, one may indeed construct (currently ad hoc) models which deplete ${}^7\text{Li}$ by a factor ≈ 2 in such stars, while respecting all other observations [29, 30]. Second, it is possible that the lithium problem points directly towards physics beyond the SBBN model, possibly connected to the production of the dark matter (cf. Section 7).

3.5. ${}^6\text{Li}$ and ${}^9\text{Be}$

The isotope of ${}^6\text{Li}$ is usually not associated with BBN, as its standard BBN production ${}^6\text{Li}/\text{H} \sim 10^{-14}$ is very low. However, the smallest deviations from SBBN may already lead to important cosmological ${}^6\text{Li}$ abundances. It is therefore interesting that the existence of ${}^6\text{Li}$ has been claimed in about ~ 10 low-metallicity stars [27], with, nevertheless, each of these observations only at the $2 - 4\sigma$ statistical significance level. Asplund *et al.* infer an average of ${}^6\text{Li}/{}^7\text{Li} \approx 0.044$ (corresponding to ${}^6\text{Li}/\text{H} \approx 6 \times 10^{-12}$) for their star sample, whereas Cayrel *et al.* infer ${}^6\text{Li}/{}^7\text{Li} \approx 0.052 \pm 0.019$ for the star HD84937 [31]. Such claims, if true, would be of great interest, as the inferred ${}^6\text{Li}/{}^7\text{Li}$ in very low metallicity stars is exceedingly hard to explain by cosmic ray production [32], though in situ production in stellar flares may be conceivable [33]. Moreover, the ${}^6\text{Li}$ observations seem to be consistent with a plateau structure at low metallicity as expected when originating right from BBN. However, recent work [34] has cast significant shadow over the claim of elevated ${}^6\text{Li}/{}^7\text{Li}$ ratios at low $[Z]$. Similar to ${}^7\text{Li}$, ${}^6\text{Li}$ is inferred from observations of atmospheric stellar absorption features. Unlike in the case of D and H in QALS, the absorption lines of ${}^7\text{Li}$ and ${}^6\text{Li}$ are always blended together. ${}^6\text{Li}/{}^7\text{Li}$ ratios may therefore be obtained only by observations of a minute asymmetry in the 6708 line. Such asymmetries could be due to ${}^6\text{Li}$, but may also be due to asymmetric convective motions in the stellar atmospheres. The analysis in Cayrel *et al.* [34] prefers the latter explanation.

Unlike the case of ${}^6\text{Li}$, detection of ${}^9\text{Be}$ in many stars at low metallicities is not controversial. Observations of ${}^9\text{Be}$ [35, 36] are far above the $O(10^{-18})$ SBBN prediction, and exhibit linear correlation with oxygen, clearly indicating its secondary (spallation) origin [37]. The lowest level of detected ${}^9\text{Be}/\text{H}$ is at $\sim \text{few} \times 10^{-14}$, which translates into the limit on the primordial fraction at 2×10^{-13} [38], assuming no significant depletion of ${}^9\text{Be}$ in stellar atmospheres.

4. Cascade nucleosynthesis from energy injection

The possibility that BBN may be significantly perturbed by the presence of energetic, non-thermal SM particles in the plasma has first received detailed attention in the 1980s [40, 41, 42, 43, 44, 45, 46, 47]. Though much of the pioneering work had been done, only recently the first fully realistic calculations of coupled thermal nuclear reactions and non-energetic phenomena have been presented [48, 49, 50, 51]. Energetic particles may be injected as products of the decay or annihilation of relic non-SM particles, or

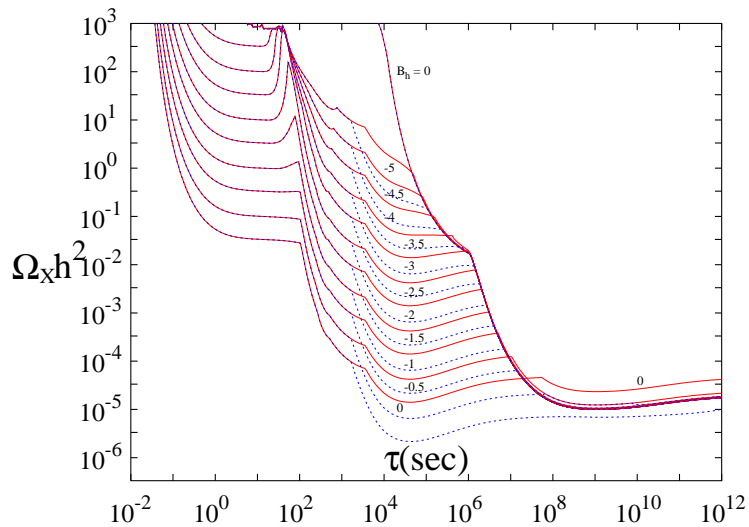


Figure 1. Constraints on the abundance $\Omega_X h^2$ of relic particles decaying at τ_X assuming $M_X = 100$ GeV for the particle mass. The most stringent limits are given, from early to late times, by ${}^4\text{He}$, D, ${}^6\text{Li}$, and ${}^3\text{He}/\text{D}$ overproduction, respectively. The various lines are for different $\log_{10} B_h$, as labeled, where B_h is the hadronic branching ratio. From Ref. [39].

via perhaps more exotic mechanisms such as evaporation of primordial black holes or supersymmetric Q-balls. The injected energetic photons γ 's, electron/positrons e^\pm 's, neutrinos ν 's, muons μ^\pm 's, pions π 's, nucleons and antinucleons N 's and \bar{N} 's, gauge bosons Z 's and W^\pm 's, etc. may be considered as the "cosmic rays" of the early Universe. In contrast to their present day counterparts, and with the exception of neutrinos, these early cosmic rays thermalize rapidly within a small fraction of the Hubble time $H^{-1}(T)$ for all cosmic temperatures above $T \sim 1$ eV. This, of course, happens only after all unstable species (i.e. π 's, μ 's, Z 's and W^\pm 's) have decayed leaving only γ 's, e^\pm 's, ν 's and N 's. Many of the changes in BBN light-element production occur during the course of this thermalization. One often distinguishes between hadronically (π 's, N 's, and \bar{N} 's) and electromagnetically (γ 's, e^\pm 's) interacting particles, mainly because the former may change BBN yields at times as early as $\tau \gtrsim 0.1$ sec (i.e. $T \lesssim 3$ MeV), whereas the latter only have impact for $\tau \gtrsim 10^5$ sec (i.e. $T \lesssim 3$ keV). In the following we summarize the most important interactions and outline the impact of such particles on BBN. For hadronically interacting particles these effects include:

- (i) π^\pm 's may cause charge exchange, i.e. $\pi^- + p \rightarrow \pi^0 + n$ between $1 \text{ MeV} \gtrsim T \gtrsim 300 \text{ keV}$ thereby creating extra neutrons after n/p freezeout and increasing the helium mass fraction Y_p .
- (ii) Antinucleons \bar{N} injected in the primordial plasma preferentially annihilate on protons, thereby raising the effective n/p -ratio and increasing Y_p .
- (iii) At higher temperatures, neutrons n 's completely thermalize through magnetic moment scattering on e^\pm ($T \gtrsim 80 \text{ keV}$), whereas protons p 's do so through Coulomb

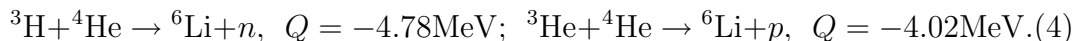
interactions with e^\pm and Thomson scattering off CMBR photons ($T \gtrsim 20$ keV). Any extra neutrons at $T \sim 40$ keV may lead to an important depletion of ${}^7\text{Be}$.

- (iv) At lower temperatures, both, energetic neutrons and protons may spall ${}^4\text{He}$, e.g. $n + {}^4\text{He} \rightarrow {}^3\text{H} + p + n + (\pi\text{'s})$, or $n + {}^4\text{He} \rightarrow \text{D} + p + 2n + (\pi\text{'s})$. Both reactions are important as they may either increase the ${}^2\text{H}$ abundance or lead to ${}^6\text{Li}$ formation via the secondary non-thermal reactions of energetic ${}^3\text{H}({}^3\text{He})$ on ambient α 's.

The main features of electromagnetic injection are:

- (i) Energetic γ 's may pair-produce on CMBR photons, i.e. $\gamma + \gamma_{\text{CMBR}} \rightarrow e^- + e^+$ as long as their energy is above the threshold $E_C \approx m_e^2/22T$ for this process. The created energetic e^\pm in turn inverse Compton scatter, i.e. $e^\pm + \gamma_{\text{CMBR}} \rightarrow e^\pm + \gamma$, to produce further γ 's. Interactions with CMBR photons completely dominate interactions with matter due to the exceedingly small cosmic baryon-to-photon ratio η .
- (ii) Only when $E_\gamma \lesssim E_C$ do interactions with matter become important. These include Bethe-Heitler pair production $\gamma + p({}^4\text{He}) \rightarrow p({}^4\text{He}) + e^+ + e^-$ and Compton scattering $\gamma + e^- \rightarrow \gamma + e^-$ off plasma electrons, as well as photodisintegration (see below).
- (iii) A small fraction of γ 's with $E_\gamma \lesssim E_C$ may photodisintegrate first D at $T \lesssim 3$ keV, when E_C becomes larger than $E_b^{\text{D}} \approx 2.2$ MeV, the D binding energy, and later ${}^4\text{He}$, at $T \lesssim 0.3$ keV since $E_b^{{}^4\text{He}} \approx 19.8$ MeV. Such processes may cause first, D destruction, and later, D and ${}^3\text{He}$ production, and more importantly ${}^3\text{He}/\text{D}$ overproduction. They may also lead to ${}^6\text{Li}$ production.

In the context of non-thermal energy injection related to particle dark matter, there are two very important processes that have profound impact on ${}^6\text{Li}$ and ${}^7\text{Li}$ abundances and deserve further comments. Energetic ${}^3\text{He}$ and ${}^3\text{H}$ produced via electromagnetic or hadronic energy injection (*i.e.* via spallation or photodisintegration) provide the possibility of efficient production of ${}^6\text{Li}$ via the non-thermal nuclear reactions on thermal ${}^4\text{He}$:



For energies of projectiles ~ 10 MeV, the cross sections for these nonthermal processes are on the order of 100 mbn, and indeed 10^7 times larger than the SBBN cross section for producing ${}^6\text{Li}$. This enhancement figure underlines the ${}^6\text{Li}$ sensitivity to non-thermal BBN, and makes it an important probe of energy injection mechanisms in the early Universe.

Another important aspect of the nonthermal BBN is the possibility to alleviate the tension between the Spite plateau value and the predicted abundance of ${}^7\text{Li}$, *e.g.* "solve the ${}^7\text{Li}$ problem". To achieve that the energy injection should occur in the temperature interval $60 \text{ keV} \gtrsim T \gtrsim 30 \text{ keV}$, *i.e.* during or just after ${}^7\text{Be}$ synthesis. The essence of this mechanism consists in the injection of $\gtrsim 10^{-5}$ neutrons per baryon that will enhance

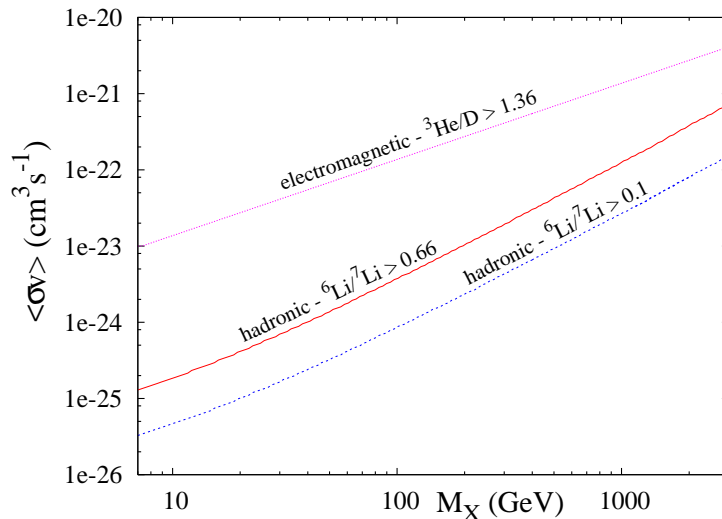
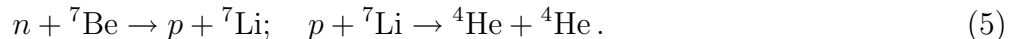


Figure 2. Upper bound on the annihilation cross section of particle dark matter of mass M_X from BBN. Here the upper line assumes annihilation into only electromagnetically interacting particles, whereas the two lower lines assume annihilation into a light quark-anti-quark pair. Adopted limits on the light element abundances are as indicated in the figure.

${}^7\text{Be} \rightarrow {}^7\text{Li}$ interconversion followed by the p -destruction of ${}^7\text{Li}$ via the thermal reaction sequence [48]:



Note that this is the same mechanism that depletes ${}^7\text{Be}$ in SBBN, but with elevated neutron concentration due to the hadronic energy injection. This mechanism of depleting ${}^7\text{Be}$ is tightly constrained by the deuterium abundance, as extra neutrons could easily overproduce D.

Fig. 1 summarizes constraints on abundance vs lifetime of relic decaying particles. It is convenient to measure the abundance in terms of $\Omega_X h^2$, the present day fraction of total energy density if these particles were to remain stable. This quantity relates to the in the literature frequently used $\zeta = n_X M_X / s$ via $\zeta = 3.6639 \times 10^{-9} \text{GeV} \Omega_X h^2$ where n_X is particle number density, M_X is particle mass, and s is entropy. It is seen that constraints get increasingly more stringent when the lifetime τ_X increases, implying also, that under generic circumstances, the production of dark matter X (with $\Omega_X h^2 \sim 0.1$) by the decay of a parent particle $Y \rightarrow X + \dots$ at $\tau_X \gg 10^3 \text{sec}$ is extremely problematic, if at all possible.

5. Residual dark matter annihilation during BBN

Many dark matter candidates X may be ultimately visible in our Galaxy due to the cosmic rays they inject induced by residual XX self-annihilations. This is, for example, the case for supersymmetric neutralinos, provided that their annihilation products

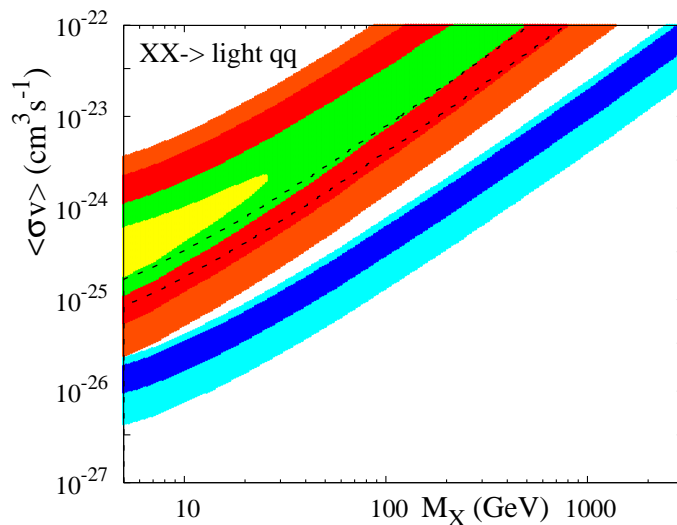


Figure 3. Dark matter annihilation rate versus dark matter mass. The blue band shows parameters where ${}^6\text{Li}$ due to residual dark matter annihilation may account for the ${}^6\text{Li}$ abundance as inferred in HD84937 (${}^6\text{Li}/{}^7\text{Li} \approx 0.014 - 0.09$ at $2\text{-}\sigma$), whereas the orange-red-green-yellow region shows where ${}^7\text{Li}$ is efficiently destroyed i.e. ${}^7\text{Li}/\text{H} < 1.5, 2, 3$, and 4×10^{-10} , respectively. Above the lower (upper) dashed line D/H exceeds 4×10^{-5} (5.3×10^{-5}), such that parameter space above the upper dashed line is ruled out by D overproduction. Scenarios between this line and the upper edge of the blue band are problematic since severely overproducing ${}^6\text{Li}$. Dark matter annihilation into light quarks has been assumed.

can be distinguished from astrophysical backgrounds. Residual annihilation events in the early Universe may also be of importance as they may lead to cosmologically significant ${}^6\text{Li}$ abundances [52] induced by the non-thermal nuclear reaction discussed in Section 4. Given an X annihilation rate $\langle\sigma v\rangle$ and X -density n_X one may determine the approximate fraction f_X of X particles which annihilate in the early Universe at temperature T

$$f_X \approx \frac{1}{n_X} \frac{dn_X}{dt} \Delta t_H \approx \langle\sigma v\rangle \frac{n_X}{s} s H^{-1} \quad (6)$$

where $\Delta t_H \approx H^{-1} = (90 M_{pl}^2 / \pi^2 g T^4)^{1/2}$ is the characteristic Hubble time at T , g is the appropriate particle statistical weight, $s = 4\pi^2/90 g T^3$ is radiation entropy, and $\langle\dots\rangle$ denotes a thermal average, which can be taken once the velocity dependence of σv is specified. Many scenarios for the production of dark matter envision a stable self-annihilating particle, typically a weakly-interacting massive particle or WIMP, whose final asymptotic abundance is given by its annihilation rate. Straightforward considerations of thermal WIMP freeze-out require the annihilation rate at $T_f^{th} \simeq 0.05 m_X$ to be $\langle\sigma v\rangle_f^{th} \approx 1 \text{pb}n \times c = 3 \times 10^{-26} \text{cm}^3 \text{s}^{-1}$ if the X -particle is to be the dominant component of dark matter, $\Omega_X h^2 \approx 0.1$. Less straightforward but still plausible scenarios that include the non-thermal production of dark matter, *e.g.* via evaporation of Q-balls and/or decay of relic particles $Y \rightarrow X + \dots$ with subsequent X self-annihilation, may

require $\langle\sigma v\rangle_f$ well in excess of $(\sigma v)_f^{th}$ for $\Omega_X h^2 \approx 0.1$. We concentrate on the WIMP example, and parametrize the velocity dependence of $\langle\sigma v\rangle$ by $\langle\sigma v\rangle = (\sigma v)_0 S(v)$, with the chosen normalization $(\sigma v)_0 = \langle\sigma v\rangle_f$. We are interested in finding the fraction of annihilating WIMP particles at $T < 10$ keV, a temperature scale below which ${}^6\text{Li}$ is no longer susceptible to nuclear burning (destruction). Exploiting (6) at the freeze-out temperature T_f , where $f_X(T_f) \approx 1$, as well as at an arbitrary other $T \ll T_f$, we obtain

$$f_X(T) \approx \left(\frac{g(T)}{g(T_f)}\right)^{1/2} \left(\frac{T}{T_f}\right) \frac{\langle S(v)\rangle_T}{\langle S(v)\rangle_{T_f}} \quad (7)$$

for $f_X \ll 1$. Several generic options are possible for the temperature scaling of the the S -ratio in (7). If the s -wave annihilation is mediated by short-distance physics and occurs away from sharp narrow resonances, $\langle S(v)\rangle_T = \langle S(v)\rangle_{T_f} = 1$, where the second equality is due to our chosen normalization. Using this conservative assumption and Eq. (7), for a WIMP of mass $M_X = 100$ GeV, so that $g(T)/g(T_f) \simeq 0.1$, one finds that only a small fraction, $f_X \approx 6 \times 10^{-7}$, of X -particles has a chance to annihilate at $T \simeq 10$ keV and below. Nevertheless, even this tiny fraction is still sufficient to produce a ${}^6\text{Li}$ abundance of ${}^6\text{Li}/\text{H} \approx 1.6 \times 10^{-12}$.

Existence of attractive Coulomb-like force of some strength α' in the WIMP sector may lead to a significant enhancement of annihilation at low temperatures/velocities[53], possibly leading to a much higher yield of ${}^6\text{Li}$. In this case the Sommerfeld-like scaling $\sigma v \sim (\pi\alpha'/v)[1 - \exp(-\pi\alpha'/v)]^{-1}$, enhances the annihilation at small $v \lesssim \pi\alpha'$, i.e. $\langle S(v)\rangle_T \simeq \pi\alpha'/v$. This leads to a $\sim T^{-1/2}$ scaling of $\langle S(v)\rangle_T$ in (7) when X -particles are still in thermal equilibrium with the plasma. After they have dropped out of thermal equilibrium, $\langle S(v)\rangle_T$ falls even more rapidly as $\sim T^{-1}$, with the net effect that weak mass scale X -particles usually have much smaller velocities at the end of BBN than in the Milky Way. Similarly, the presence of narrow resonances just above the XX annihilation threshold may drastically boost the annihilation at low energies. Both mechanisms of enhancing the annihilation have been widely discussed (see *e.g.* [54]) in an attempt to link some cosmic-ray anomalies to dark matter annihilation, as for example an elevated positron fraction $e^+/(e^- + e^+)$ observed by PAMELA instrument [55].

Keeping the annihilation rate as a free parameter, Fig. 2 shows the upper limit on the effective annihilation cross section imposed by BBN. Here electromagnetically- (upper line) and hadronically- (lower lines) annihilating particle DM has been considered. The former is mostly constrained by overproduction of ${}^3\text{He}/\text{D}$ at $T \approx 0.1$ keV, while the latter by ${}^6\text{Li}/{}^7\text{Li}$ overproduction at $T \approx 10$ keV, such that the effective annihilation cross section refer to $\langle\sigma v\rangle$ at those temperatures. Due to the possibility of ${}^6\text{Li}$ destruction a fairly conservative ${}^6\text{Li}/{}^7\text{Li} < 0.66$ constraint has also been considered. It is seen that much ${}^6\text{Li}$ may be produced by hadronic annihilations. Fig. 3 shows dark matter parameters which lead to the production of a ${}^6\text{Li}/{}^7\text{Li}$ ratio as claimed to be observed in the star HD84937 at 1σ and 2σ (dark blue and light blue), respectively. Here a completely hadronic $XX \rightarrow q\bar{q}$ annihilation has been employed, an assumption which could be further confronted with the constraints on antiproton fluxes in our galaxy.

Electromagnetic annihilations, as often implied in recent dark-matter interpretations of PAMELA[55], may also lead to ${}^6\text{Li}$, but only annihilations below $T \lesssim 0.3 \text{ keV}$ may do so efficiently. Note, that the figure already implicitly assumes a factor $\sim 3 - 4$ stellar destruction of ${}^7\text{Li}$ (and ${}^6\text{Li}$) to solve the lithium problem. It is therefore found that weak-scale mass dark matter particles, if fairly light, and if annihilating into hadronically interacting particles, may account for all of the observed ${}^6\text{Li}$ in HD84937. The figure also shows by the orange-red-green-yellow areas the dark matter parameters which would lead to a significant ${}^7\text{Li}$ destruction due to residual dark matter annihilations, with the nuclear destruction mechanism described in the previous section. Since those regions are much above the ${}^6\text{Li}$ band, the possibility of a factor of 2 or more depletion in ${}^7\text{Li}$ is severely constrained by ${}^6\text{Li}$ overproduction. We note in passing that our constraints are significantly more conservative than those found in Ref. [56]. It is intriguing to realize that primordial ${}^6\text{Li}$ production by residual (hadronic) dark matter annihilations dominates standard BBN ${}^6\text{Li}$ production for annihilation rates as small as $\langle\sigma v\rangle \sim 10^{-27} \text{ cm}^3 \text{ s}^{-1}$, well below $\langle\sigma v\rangle_f^{th}$. It is thus possible that in the most primeval gas clouds and in the oldest stars the bulk of ${}^6\text{Li}$ is due to dark matter annihilations. Unfortunately, ${}^6\text{Li}$ abundances as low as ${}^6\text{Li}/\text{H} \lesssim 10^{-12}$ are difficult to observe.

6. Catalyzed BBN (CBBN)

The idea of particle physics catalysis of nuclear reactions goes back to the 1950s, and muon-catalyzed fusion has been a subject of active theoretical and experimental research in nuclear physics. In recent years there has been a significant interest towards a possibility of nuclear catalysis by hypothetical negatively charged particles that live long enough to participate in nuclear reactions at the BBN time [57, 58, 59, 51, 60, 61, 62, 63, 64, 65, 66, 38, 67] (see also Ref. [68, 69, 70] for earlier work on the subject). An essence of the idea is very simple: a negatively charged massive particle that we call X^- gets into a bound state with the nucleus of mass m_N and charge Z , forming a large compound nucleus with the charge $Z - 1$, mass $M_X + m_N$, and the binding energy in the $O(0.1 - 1) \text{ MeV}$ range. Once the bound state is formed, the Coulomb barrier is reduced signalling a higher "reactivity" of the compound nucleus with other nuclei. But what proves to be the most important effects of catalysis, are new reaction channels which may open up and avoid SBBN-suppressed production mechanisms [57], *e.g.* Eq. (3), thus clearing path to synthesis of elements such as ${}^6\text{Li}$ and ${}^9\text{Be}$. Although in this chapter we discuss the catalysis by negatively charged heavy relics, this is not the only option for CBBN, as for example, strongly interacting relics may also participate and catalyze certain nuclear reactions.

Although the connection between dark matter and CBBN is not immediate - after all the dark matter may not be charged - it is possible that dark matter particles do have a relatively long-lived charged counterpart. One example of this kind is supersymmetry with the lightest supersymmetric particle (LSP) the gravitino and the next-to-LSP (NLSP) a charged slepton to be examined in the next section. In that case

bound state	a_0 [fm]	$ E_b $ [keV]	T_0 [keV]
pX^-	29	25	0.6
${}^4\text{He}X^-$	3.63	346	8.2
${}^7\text{Be}X^-$	1.03	1350	32
${}^8\text{Be}X^-$	0.91	1430	34

Table 1. Properties of the bound states: Bohr radius $a_0 = 1/(Z\alpha m_N)$, binding energies E_b , calculated for realistic charge radii, and “photo-dissociation decoupling” temperatures T_0 .

the decay of the NLSP is tremendously delayed by the smallness of the gravitino-lepton-slepton coupling $\sim G_N^{1/2}$. Another example in the same vein is the nearly degenerate stau-neutralino system, in which case the longevity of the charged stau against the decay to the dark matter neutralino is ensured as long as the mass splitting of the stau-neutralino system is below 100 MeV. Both, the gravitino and neutralino in these two examples represent viable dark matter candidates. A very important aspect of CBBN is that the abundance of charged particles before they start decaying is given by their annihilation rate at freeze-out. In most of the models their abundance is easily calculable, and if no special mechanisms are introduced to boost the annihilation rate, the abundance of charged particles per nucleon is not small, and in the typical ballpark of $Y_X \sim (0.001 - 0.1) \times m_X/\text{TeV}$.

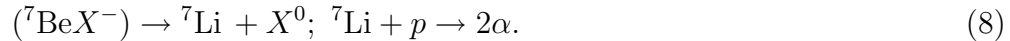
Properties of the bound states.

For light nuclei participating in BBN, we can assume that the reduced mass of the nucleus- X^- system is well approximated by the nuclear mass, so that the binding energy is given by $Z^2\alpha^2 m_A/2$ when the Bohr orbit is larger than the nuclear radius. It turns out that this is a poor approximation for all nuclei heavier than $A = 4$, and the effect of the finite nuclear charge radius has to be taken into account. In Table 1 we give the binding energies, as well as the recombination temperature, defined as the temperature at which the photodissociation rate of bound states becomes smaller than the Hubble expansion rate. Below these temperatures bound states are practically stable, and the most important benchmark temperatures for the CBBN are the $T \sim 30, 8, 0.5$ keV, when (${}^7\text{Be}X^-$), (${}^4\text{He}X^-$), and (pX^-) can be formed without efficient suppression by the photodissociation processes. It is important to emphasize that these properties of the bound states are generic to any CBBN realization: *i.e.* they are completely determined by the charge of X^- and electromagnetic properties of nuclei, and thus are applicable to SUSY or non-SUSY models alike. It is also important to note that the (${}^8\text{Be}X^-$) compound nucleus is stable, which may open the path to synthesis of $A > 8$ elements in CBBN.

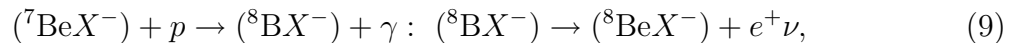
Catalysis at 30 keV: suppression of ${}^7\text{Be}$.

When the Universe cools to temperatures of 30 keV, the abundances of deuterium, ${}^3\text{He}$, ${}^4\text{He}$, ${}^7\text{Be}$ and ${}^7\text{Li}$ are already close to their freeze-out values, although several nuclear processes remain faster than the Hubble rate. At these temperatures, a

negatively charged relic can get into bound states with ${}^7\text{Be}$ and form a $({}^7\text{Be}X^-)$ composite object. Once this object is formed, some new destruction mechanisms for ${}^7\text{Be}$ appear. For models with weak currents connecting nearly mass-degenerate X^- - X^0 states, a very fast internal conversion followed by the p -destruction of ${}^7\text{Li}$:



When $X^- \rightarrow X^0$ is energetically disallowed the destruction of ${}^7\text{Be}$ can be achieved via the following chain:



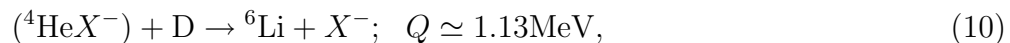
which is much enhanced by the atomic resonances in the $({}^7\text{Be}X^-)$ system [61].

The rates for both mechanisms may be faster than the Hubble rate, possibly leading to a sizable suppression of ${}^7\text{Be}$ abundance *if* $({}^7\text{Be}X^-)$ bound states are efficiently forming. In other words, $({}^7\text{Be}X^-)$ serves as a bottleneck for the CBBN depletion of ${}^7\text{Be}$. The recombination rate per ${}^7\text{Be}$ nucleus leading to $({}^7\text{Be}X^-)$ is given by the product of recombination cross section and the concentration of X^- particles. It can be easily shown that for $Y_X < 0.01$ the recombination rate is too slow to lead to a significant depletion of ${}^7\text{Be}$. Detailed calculation of recombination rate and numerical analyses of the CBBN at 30 keV [61, 66] find that the suppression of ${}^7\text{Be}$ by a factor of 2 is possible for $Y_X \geq 0.1$ if only mechanism (9) is operative, and for $Y_X \geq 0.02$ if the internal conversion (8) is allowed.

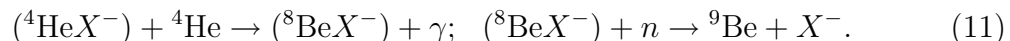
Catalysis at 8 keV: enhancement of ${}^6\text{Li}$ and ${}^9\text{Be}$.

As the Universe continues to cool below 10 keV, an efficient formation of $({}^4\text{He}X^-)$ bound states becomes possible. With the reasonable assumption of $Y_X < Y_{\text{He}}$ the rate of formation of bound states per X^- particle is given by the recombination cross section and the concentration of the helium nuclei. Numerical analysis of recombination reveals that at $T \simeq 5$ keV about 50% of available X^- particles will be in bound states with ${}^4\text{He}$ [57].

As soon as $({}^4\text{He}X^-)$ is formed, new reaction channels open up. In particular, a photonless thermal production of ${}^6\text{Li}$ becomes possible



which exceeds the SBBN production rate by \sim six orders of magnitude. The production of ${}^9\text{Be}$ may also be catalyzed, possibly by many orders of magnitude relative to the SBBN values, with the following thermal nuclear chain [65]:



Both reactions at these energies are dominated by the resonant contributions, although the efficiency of the second process in (11) is not fully understood.

Current estimates/calculations of the CBBN rates are used to determine the generic constraints on lifetimes/abundances of charged particles. The essence of these limits is displayed in Figure 4, which shows that for typical X^- abundances the lifetime of the charged particles would have to be limited by a few thousand seconds! This is the main

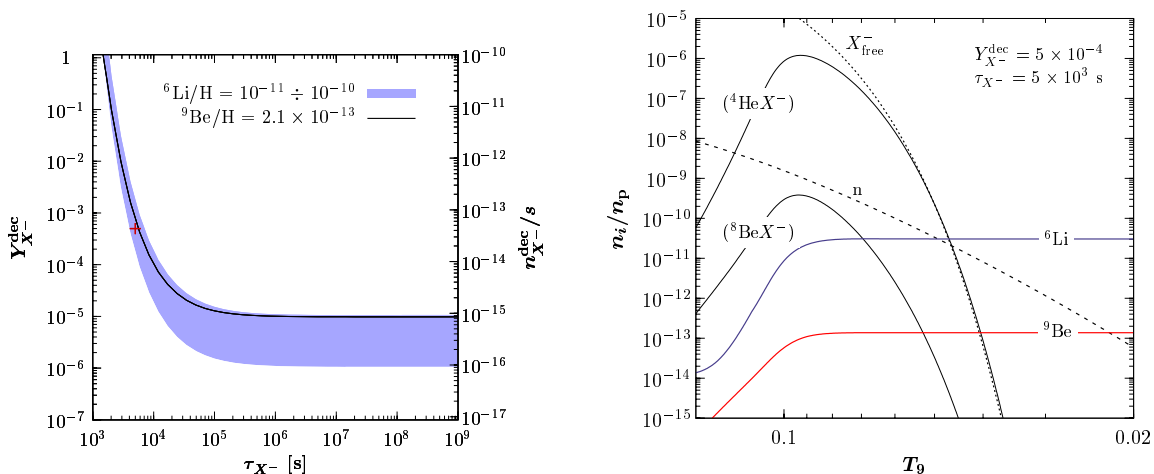


Figure 4. Left panel shows CBBN constraints on the abundance vs lifetime of X^- . The red cross corresponds to a point in the parameter space, for which the temporal development of ${}^6\text{Li}$ and ${}^9\text{Be}$ is shown in the right panel, following Ref. [38].

conclusion to be learned from CBBN. Note that while, to lowest order, non-thermal BBN is sensitive to the energy density of decaying particles, the CBBN processes are controlled by the number density of X^- , which underlines the complimentary character of these constraints. In some models, where both catalysis and cascade nucleosynthesis occur, catalysis dominates cascade production of ${}^6\text{Li}$ for all particles with hadronic branching ratio $B_h \lesssim 10^{-2}$ [64], whereas ${}^7\text{Li}$ destruction is usually dominated by cascade effects unless $B_h \lesssim 10^{-4}$. ${}^9\text{Be}$ production, on the other hand, is conceivable only through catalysis.

Catalysis below 1 keV and nuclear uncertainties

Finally we comment on the possibility of (pX^-) catalysis of nuclear reactions, discussed in Refs. [69, 63]. Although it is conceivable that the absence of the Coulomb barrier for this compound nucleus may lead to significant changes of SBBN/CBBN predictions, in practice it turns out that in most cases (pX^-) -related mechanisms are of secondary importance. The large radius and shallow binding of this system leads to a fast charge-exchange reaction on helium, $(pX^-) + {}^4\text{He} \rightarrow ({}^4\text{He}X^-) + p$, that reduces the abundance of (pX^-) below 10^{-6} relative to hydrogen, as long as $Y_{X^-} \lesssim Y_{4\text{He}}$, making further reactions inconsequential for any observable element [38]. In the less likely case, $Y_{X^-} \gtrsim Y_{4\text{He}}$, significant late-time processing due to (pX^-) bound states may still occur. Such late time BBN, nevertheless, typically leads to observationally unacceptable final BBN yields.

Unlike in the SBBN case and even in cascade nucleosynthesis that utilizes mostly measured nuclear reaction rates, CBBN rates cannot be measured in the laboratory, and significant nuclear theory input for the calculation of the reaction rates is required. However, since the X^- participates only in electromagnetic interactions, such calculations are feasible, and dedicated nuclear theory studies [60] in this direction has already commenced. The reaction rates for some CBBN processes, such as (9) and (10)

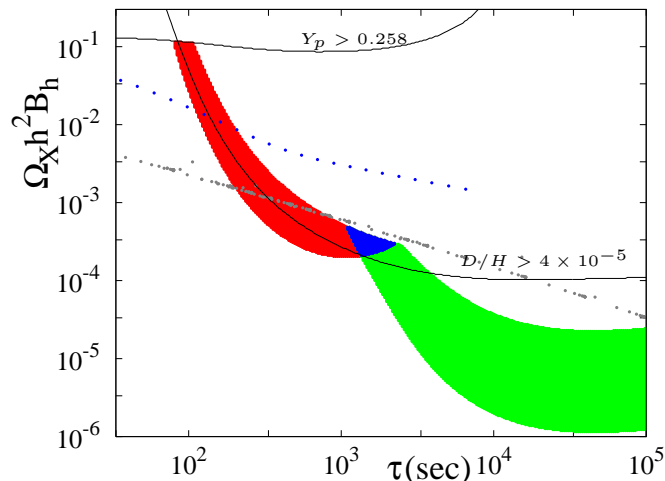


Figure 5. Parameter space in the relic decaying particle abundance times hadronic branching ratio B_h , i.e. $\Omega_X h^2 B_h$, and life time τ_X plane, where ^7Li is significantly reduced (red and blue) and ^6Li is efficiently produced (green and blue). See text for further details. From Ref. [71].

are already known within a factor of 2 accuracy, and the detailed calculations for the ^9Be synthesis are underway [67].

7. Dark Matter Production during BBN: NLSP \rightarrow LSP example

Dark matter particles may be produced by the decay of relic parent particles X during BBN. Examples, well-studied by different groups, include the production of gravitino-LSP dark matter by NLSP decays (often charged sleptons or neutralinos) or production of neutralino dark matter by heavier gravitinos. Other conceivable possibilities include the production of superweakly interacting Kaluza-Klein dark matter, and more generally the cascade decays to any superweakly interacting dark matter candidates. In case of charged NLSP decays, both nonthermal and CBBN processes must be accounted for. In the framework of gravitino-LSP/stau-NLSP the lifetime of the charged slepton in the limit of $m_{\tilde{G}} \ll M_{\text{NLSP}}$ is given by

$$\tau_{\text{NLSP}} \approx 2.4 \times 10^4 \text{ sec} \times \left(\frac{M_{\text{NLSP}}}{300 \text{ GeV}} \right)^{-5} \left(\frac{m_{\tilde{G}}}{10 \text{ GeV}} \right)^2, \quad (12)$$

where M_{NLSP} and $m_{\tilde{G}}$ denote NLSP and gravitino mass, respectively.

It becomes exceedingly more difficult with increasing τ_X to obtain observational consistency with inferred primordial abundances (cf. Fig. 1). BBN therefore plays an important role in constraining such scenarios (cf. Sections 4 and 6). However, BBN may not only constrain, but also favor particular scenarios, if current discrepancies with ^6Li and ^7Li abundances are to be taken seriously. Both trends, the reduction of ^7Li and the production of ^6Li via mechanisms described in Sections 4 and 6, are seen in Fig. 5. There the red area shows decaying particle parameter space resulting in more than a factor of 2 suppressed ^7Li abundance relative to the SBBN prediction, and the green area shows

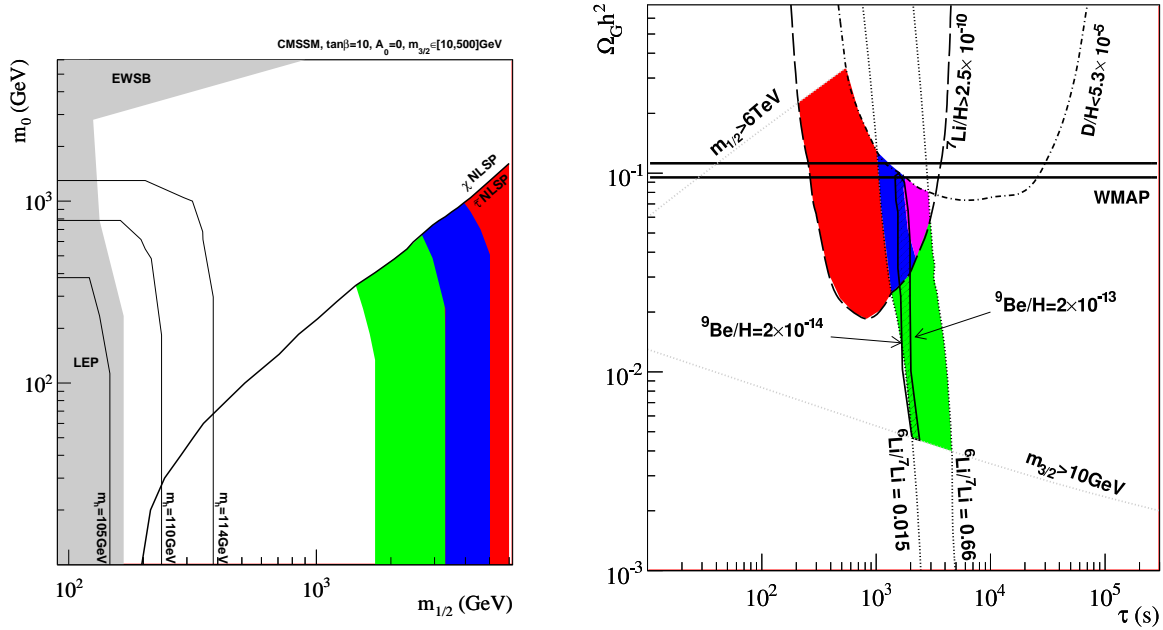


Figure 6. Parameter space in the CMSSM which may impact the primordial ${}^7\text{Li}$ and/or ${}^6\text{Li}$ abundances with the color coding essentially as in Fig. 5. Left: unifying scalar soft mass m_0 versus gaugino soft mass $m_{1/2}$; Right: gravitino abundance $\Omega_{\tilde{G}} h^2$ versus NLSP life time τ . From Ref. [71].

regions where significant ${}^6\text{Li}$ production ($0.015 \lesssim {}^6\text{Li}/{}^7\text{Li} \lesssim 0.3$) occurs. In the overlap of these areas, the blue area, both effects may be achieved simultaneously [48, 51, 72]. Fig. 5 also shows the prediction of supersymmetric scenarios with the gravitino-LSP, for some representative values of other supersymmetric mass parameters. In particular, the grey dots show predictions of stau NLSPs with gravitino LSPs of mass $m_{\tilde{G}} = 50 \text{ GeV}$ within the so-called constrained minimal supersymmetric SM (CMSSM), whereas the blue dots show the case of neutralino NLSPs decaying into $m_{\tilde{G}} = 100 \text{ MeV}$ gravitino LSPs within the gauge-mediated supersymmetry breaking scenario. It is seen that both scenarios naturally cross the region of “ ${}^7\text{Li}$ destruction”. The assumption underlying these models is a thermal freeze-out abundance of the NLSP. Since this typically leads to NLSP abundances, $10^{-3} \lesssim \Omega_{\text{NLSP}} \lesssim 10^3$, and taking into account that gravitino energy density due to NLSP decays is $\Omega_{\tilde{G}} = \Omega_{\text{NLSP}} (m_{\tilde{G}}/M_{\text{NLSP}})$, the resulting $\Omega_{\tilde{G}}$ produced in such scenarios may come close to the observed dark matter density. This is particularly the case for heavy gravitinos $m_{\tilde{G}} \sim 100 \text{ GeV}$ in the CMSSM, for which a more detailed results are shown in Fig. 6. It is intriguing, and perhaps purely coincidental, that when resolving the tension between observed and predicted ${}^7\text{Li}$ abundance by staus decaying into gravitinos, the resulting gravitino abundance may account for all the dark matter. For stau decay times $\tau \approx 10^3 \text{ sec}$ it is furthermore possible to synthesize a primordial ${}^6\text{Li}$ abundance as claimed to be observed in low-metallicity stars. Moreover, though less certain, the same parameter space could also lead to an important ${}^9\text{Be}$ abundance due to catalytic effects (cf. Section 6), as indicated by the cross-hatched region in Fig. 6.

Finally, since produced by decays, gravitino dark matter in such scenarios is significantly warm, with free-streaming velocities of the same order as those of a $m \approx 3 \text{ keV}$ early freezing-out relic particle, which has important implications for the small scale structures in the present day Universe. It is therefore not impossible that some time in the future, anomalies in the primordial light elements may have been understood as signs of the dark matter. Nevertheless, independent verification by particle accelerators, such as the LHC is required. Unfortunately, scenarios as presented in Fig. 6 require staus of mass $m_{\tilde{\tau}} \gtrsim 1 \text{ TeV}$ too heavy to be produced at the LHC.

8. Conclusions

Even though the concept of Big Bang Nucleosynthesis is more than 50 yr old, it continues being relevant due to the constant progress in nuclear physics, astrophysics, and the refined quality of calculations. In this paper, we have reviewed the status of BBN, and have shown how New Physics can modify the synthesis of light element abundances. All three generic ways, extra degrees of freedom modifying the Hubble expansion during BBN, energy injection due to annihilation or decay of heavy particles, and particle catalysis of BBN reactions, are highly relevant to the physics associated with particle dark matter, or with particles intimately tied to dark matter. We have illustrated how the existing overall concordance between the predicted elemental abundances and observations lead to some very non-trivial constraints on the properties of DM particles and their companions (*e.g.* stau-gravitino system).

Perhaps even more intriguing is the current discrepancy between the observed and standard BBN predicted abundance of ${}^7\text{Li}$ at the level of 2-3. This discrepancy has firmed up since the last unknown SBBN parameter, the baryon-to-photon ratio, has been determined with better than 5% accuracy by recent high-precision CMB experiments. At this moment it is premature to tell how the ${}^7\text{Li}$ problem is resolved, but it is nonetheless intriguing that certain models with unstable particles are capable of alleviating this discrepancy. Hopefully, the continuing improvement of observational determination of primordial light element abundances, as well as the future breakthroughs in electroweak scale particle physics would help to solve this important problem.

References

- [1] Dunkley J *et al.* (WMAP) 2008 (*Preprint* 0803.0586)
- [2] Malaney R A and Mathews G J 1993 *Phys. Rept.* **229** 145–219
- [3] Sarkar S 1996 *Rept. Prog. Phys.* **59** 1493–1610 (*Preprint* hep-ph/9602260)
- [4] Iocco F, Mangano G, Miele G, Pisanti O and Serpico P D 2008 (*Preprint* 0809.0631)
- [5] Wagoner R V, Fowler W A and Hoyle F 1967 *Astrophys. J.* **148** 3–49
- [6] Mukhanov V F 2004 *Int. J. Theor. Phys.* **43** 669–693 (*Preprint* astro-ph/0303073)
- [7] Cyburt R H, Fields B D and Olive K A 2008 (*Preprint* 0808.2818)
- [8] Nara Singh B S, Hass M, Nir-El Y and Haquin G 2004 *Phys. Rev. Lett.* **93** 262503 (*Preprint* nucl-ex/0407017)
- [9] Gyurky G *et al.* 2007 *Phys. Rev.* **C75** 035805 (*Preprint* nucl-ex/0702003)

- [10] Brown T A D *et al.* 2007 *Phys. Rev.* **C76** 055801 (*Preprint* 0710.1279)
- [11] Peimbert M, Luridiana V and Peimbert A 2007 (*Preprint* astro-ph/0701580)
- [12] Izotov Y I, Thuan T X and Stasinska G 2007 *Astrophys. J.* **662** 15–38 (*Preprint* astro-ph/0702072)
- [13] Porter R L, Ferland G J and MacAdam K B 2007 *Astrophys. J.* **657** 327–337 (*Preprint* astro-ph/0611579)
- [14] Olive K A and Skillman E D 2004 *Astrophys. J.* **617** 29 (*Preprint* astro-ph/0405588)
- [15] Fukugita M and Kawasaki M 2006 *Astrophys. J.* **646** 691
- [16] Burles S and Tytler D 1998 *Astrophys. J.* **499** 699 (*Preprint* astro-ph/9712108)
- [17] Levshakov S A, Dessauges-Zavadsky M, D’Odorico S and Molaro P 2001 (*Preprint* astro-ph/0105529)
- [18] Crighton N H M, Webb J K, Ortiz-Gill A and Fernandez-Soto A 2004 *Mon. Not. Roy. Astron. Soc.* **355** 1042 (*Preprint* astro-ph/0403512)
- [19] O’Meara J M *et al.* 2006 *Astrophys. J.* **649** L61–L66 (*Preprint* astro-ph/0608302)
- [20] Pettini M, Zych B J, Murphy M T, Lewis A and Steidel C C 2008 (*Preprint* 0805.0594)
- [21] Fields B and Sarkar S 2006 (*Preprint* astro-ph/0601514)
- [22] Steigman G 2007 *Ann. Rev. Nucl. Part. Sci.* **57** 463–491 (*Preprint* 0712.1100)
- [23] Geiss J and Gloeckler G 2007 *Space Science Reviews* **130** 5
- [24] Sigl G, Jedamzik K, Schramm D N and Berezhinsky V S 1995 *Phys. Rev.* **D52** 6682–6693 (*Preprint* astro-ph/9503094)
- [25] Ryan S G, Norris J E and Beers T C 1999 *Astrophys. J.* **523** 654–677 (*Preprint* astro-ph/9903059)
- [26] Hosford A, Ryan S G, Perez A E G, Norris J E and Olive K A 2008 (*Preprint* 0811.2506)
- [27] Asplund M, Lambert D L, Nissen P E, Primas F and Smith V V 2006 *Astrophys. J.* **644** 229–259 (*Preprint* astro-ph/0510636)
- [28] Bonifacio P *et al.* 2002 (*Preprint* astro-ph/0204332)
- [29] Richard O, Michaud G and Richer J 2005 *Astrophys. J.* **619** 538–548 (*Preprint* astro-ph/0409672)
- [30] Korn A *et al.* 2006 *Nature* **442** 657–659 (*Preprint* astro-ph/0608201)
- [31] Cayrel R, Spite M, Spite F, Vangioni-Flam E, Casse M and Audouze J 1999 *Astron. and Astrophys.* **343** 923 (*Preprint* 9901205)
- [32] Prantzos N 2005 (*Preprint* astro-ph/0510122)
- [33] Tatischeff V and Thibaud J P 2007 *Astron. and Astrophys.* **469** 265 (*Preprint* astro-ph/0610756)
- [34] Cayrel R *et al.* 2007 (*Preprint* 0708.3819)
- [35] Primas F, Asplund M, Nissen P E and Hill V 2000 (*Preprint* astro-ph/0009482)
- [36] Boesgaard A M and Novicki M C 2006 *Astrophys. J.* **641** 1122–1130 (*Preprint* astro-ph/0512317)
- [37] Fields B D, Olive K A and Vangioni-Flam E 2005 *Astrophys. J.* **623** 1083–1091 (*Preprint* astro-ph/0411728)
- [38] Pospelov M, Pradler J and Steffen F D 2008 *JCAP* **0811** 020 (*Preprint* 0807.4287)
- [39] Jedamzik K 2006 *Phys.Rev.D* **74** 103509 (*Preprint* hep-ph/0604251)
- [40] Ellis J R, Nanopoulos D V and Sarkar S 1985 *Nucl. Phys.* **B259** 175
- [41] Levitan Y L, Sobol I M, Khlopov M Y and Chechetkin V M 1988 *Sov. J. Nucl. Phys.* **47** 109–115
- [42] Dimopoulos S, Esmailzadeh R, Hall L J and Starkman G D 1988 *Astrophys. J.* **330** 545
- [43] Reno M H and Seckel D 1988 *Phys. Rev.* **D37** 3441
- [44] Dimopoulos S, Esmailzadeh R, Hall L J and Starkman G D 1989 *Nucl. Phys.* **B311** 699
- [45] Ellis J R, Gelmini G B, Lopez J L, Nanopoulos D V and Sarkar S 1992 *Nucl. Phys.* **B373** 399–437
- [46] Khlopov M Y, Levitan Y L, Sedelnikov E V and Sobol I M 1994 *Phys. Atom. Nucl.* **57** 1393–1397
- [47] Kawasaki M and Moroi T 1995 *Astrophys. J.* **452** 506 (*Preprint* astro-ph/9412055)
- [48] Jedamzik K 2004 *Phys. Rev.* **D70** 063524 (*Preprint* astro-ph/0402344)
- [49] Kawasaki M, Kohri K and Moroi T 2005 *Phys. Lett.* **B625** 7–12 (*Preprint* astro-ph/0402490)
- [50] Kawasaki M, Kohri K and Moroi T 2005 *Phys.Rev.D* **71** 083502 (*Preprint* astro-ph/0408426)
- [51] Cyburt R H, Ellis J R, Fields B D, Olive K A and Spanos V C 2006 *JCAP* **0611** 014 (*Preprint* astro-ph/0608562)

- [52] Jedamzik K 2004 *Phys. Rev.* **D70** 083510 (*Preprint astro-ph/0405583*)
- [53] Hisano J, Matsumoto S and Nojiri M M 2004 *Phys. Rev. Lett.* **92** 031303 (*Preprint hep-ph/0307216*)
- [54] Pospelov M and Ritz A 2009 *Phys. Lett.* **B671** 391–397 (*Preprint 0810.1502*)
- [55] Adriani O *et al.* 2008 (*Preprint 0810.4995*)
- [56] Hisano J, Kawasaki M, Kohri K and Nakayama K 2009 *Phys. Rev.* **D79** 063514 (*Preprint 0810.1892*)
- [57] Pospelov M 2007 *Phys. Rev. Lett.* **98** 231301 (*Preprint hep-ph/0605215*)
- [58] Kohri K and Takayama F 2007 *Phys. Rev.* **D76** 063507 (*Preprint hep-ph/0605243*)
- [59] Kaplinghat M and Rajaraman A 2006 *Phys. Rev.* **D74** 103004 (*Preprint astro-ph/0606209*)
- [60] Hamaguchi K, Hatsuda T, Kamimura M, Kino Y and Yanagida T T 2007 *Phys. Lett.* **B650** 268–274 (*Preprint hep-ph/0702274*)
- [61] Bird C, Koopmans K and Pospelov M 2008 *Phys. Rev.* **D78** 083010 (*Preprint hep-ph/0703096*)
- [62] Jittoh T *et al.* 2007 *Phys. Rev.* **D76** 125023 (*Preprint 0704.2914*)
- [63] Jedamzik K 2008 *Phys. Rev.* **D77** 063524 (*Preprint 0707.2070*)
- [64] Jedamzik K 2008 *JCAP* **0803** 008 (*Preprint 0710.5153*)
- [65] Pospelov M 2007 (*Preprint 0712.0647*)
- [66] Kusakabe M, Kajino T, Boyd R N, Yoshida T and Mathews G J 2007 (*Preprint 0711.3858*)
- [67] Kamimura M, Kino Y and Hiyama E 2008 (*Preprint 0809.4772*)
- [68] De Rujula A, Glashow S L and Sarid U 1990 *Nucl. Phys.* **B333** 173
- [69] Dimopoulos S, Eichler D, Esmailzadeh R and Starkman G D 1990 *Phys. Rev.* **D41** 2388
- [70] Rafelski J, Sawicki M, Gajda M and Harley D 1991 *Phys. Rev.* **A44** 4345
- [71] Bailly S, Jedamzik K and Moultaqa G 2008 (*Preprint 0812.0788*)
- [72] Cumberbatch D *et al.* 2007 *Phys. Rev.* **D76** 123005 (*Preprint 0708.0095*)